

# Novel techniques for improvement the NNetEn entropy calculation for short and noisy time series

**Hanif Heidari<sup>1\*</sup> and Andrei Velichko<sup>2</sup>**

<sup>1</sup>Department of Applied Mathematics, Damghan University, Damghan, Iran

<sup>2</sup>Institute of Physics and Technology, Petrozavodsk State University, 31 Lenina Str., 185910 Petrozavodsk, Russia

\*Corresponding author: heidari@du.ac.ir; Tel.: +98-23-35220092

## Abstract

Entropy is a fundamental concept of information theory. It is widely used in the analysis of analog and digital signals. Conventional entropy measures have drawbacks, such as sensitivity to the length and amplitude of time series and low robustness to external noise. Recently, the NNetEn entropy measure has been introduced to overcome these problems. The NNetEn entropy uses a modified version of the LogNNet neural network classification model. The algorithm contains a reservoir matrix with  $N = 19625$  elements, which the given time series should fill. Many practical time series have less than 19625 elements. Against this background, this paper investigates different duplicating and stretching techniques for filling to overcome this difficulty. The most successful technique is identified for practical applications. The presence of external noise and bias are other important issues affecting the efficiency of entropy measures. In order to perform meaningful analysis, three time series with different dynamics (chaotic, periodic, and binary), with a variation of signal-to-noise ratio (SNR) and offsets, are considered. It is shown that the error in the calculation of the NNetEn entropy does not exceed 10% when the SNR exceeds 30 dB. This opens the possibility of measuring the NNetEn of experimental signals in the presence of noise of various nature, white noise, or 1/f noise, without the need for noise filtering.

Keywords: entropy, NNetEn, time series, neural network, short length signal, signal to noise ratio, offset.

## 1. Introduction

Entropy-based methods are efficient tools for analyzing dynamic signals. These methods are widely used in medical diagnosis, fault detection, image processing, and speech recognition. Researchers are actively applying entropy measures in real-world applications. Li et al. used multiscale symbolic fuzzy entropy for fault detection in rotating machinery [1]; Minhas et al. used the weighted entropy method for bearing fault detection [2]; Ai et al. used fusion information entropy for rolling bearing fault detection in aircraft engines [3]; Ra et al. evaluated the permutation entropy of EEG signals for early diagnosis of epileptic seizures [4]; Zavala-Yoe et al. drew on multiscale entropy to study Doose and Lennox-Gastaut syndromes in children [5]; Benedetto et al. used Shannon entropy to model the flows between different financial time series [6]; Silva et al. investigated the predictability of monthly precipitation time series using permutation entropy; Nie et al. introduced a generalized entropy measure for image segmentation [7]; and Oludehinwa et al. investigated the relationship between the degree of complexity of magnetospheric dynamics and various categories of geomagnetic storms using the maximum Lyapunov exponent and the approximate entropy measure [8].

The effect of noise on the entropy value is one of the most important factors when comparing different entropy measures [9]. The Kolmogorov-Sinai entropy and the correlation integral algorithm are inefficient in the presence of noise [10]. The permutation entropy measure is unstable in the presence of noise [11]. Therefore, reducing the effects of noise has become a popular research topic. Xie used fuzzy spectrum entropy analysis to denoise biomedical signals [12]; Chatterjee et al. applied pattern recognition entropy to the time series of ion current chromatograms to reduce the effect of an existing noise from chemical and electronic sources [13]; Na et al. drew on cross-correlation and Shannon entropy to reduce the effect of unwanted noise [14] and Wang et al. studied multi-fault feature extraction of a transmission in the presence of high noise [15]. The length of the time series is another difficulty that affects the value of entropy [9,16,17]. Conventional entropy measures are not suitable for time series analysis because they are very sensitive to the length of the time series [18,19]. Wu et al. introduced modifications to multiscale entropy to overcome imprecise entropy values [20]; and Niu and Wang analyzed the short financial time series with a modified version of multiscale entropy to overcome this difficulty [18].

Recently, Velichko and Heidari proposed a new entropy measure (NNetEn) based on the LogNNet artificial neural network [21]. The number of epochs is the only control parameter of the NNetEn algorithm that leads to more stable results than other entropy measures. Moreover, it is independent of signal amplitude and does not consider probability distribution, which distinguishes the measure from other traditional entropy measures [22]. The NNetEn algorithm requires a time series with 19625 elements. This condition is rarely met in real-world applications. The authors proposed a matrix filling method to overcome this difficulty. Their results show that NNetEn is almost stable for time series longer than 11000. In practice, it is difficult to obtain time series in the range of elements  $N = 11000-19625$ , which are most suitable for NNetEn evaluation [21]. Data obtained from financial markets [23], physical experiments [24,25], and biological or medical data [26,27] may have  $N < 11000$  elements. Against this background, the goal of this work is twofold. First, we investigate different matrix filling techniques to improve the existing method for short time series. Second, we investigate the effect of the signal-to-noise ratio (SNR) on NNetEn. The results show that the method can be applied to time series with length  $N \geq 50$ , and the error in calculating the NNetEn entropy does not exceed 10% when the SNR is more than 30 dB.

The rest of the paper is structured as follows. In Section 2, the LogNNet model and matrix padding techniques are presented. In Section 3, numerical examples are presented to investigate the efficiency of the matrix filling techniques and the effect of noise on the NNetEn measure. Finally, Section 4 is devoted to conclusions.

## 2. Methods

### 2.1. LogNNet model for entropy calculation

NNetEn is a recently introduced entropy measure based on the LogNNet model (see Figure 1) [21]. Unlike conventional entropy measures, NNetEn does not consider a probability distribution but only a control parameter. These advantageous features make NNetEn a powerful entropy measure. In the NNetEn algorithm, the MNIST-10 dataset is considered input of LogNNet, and the given time series is used to construct the reservoir matrix. In total, the matrix contains  $N_0 = 19625$  elements. In the classification phase, a feedforward artificial neural network with a layer of 25 neurons is used.

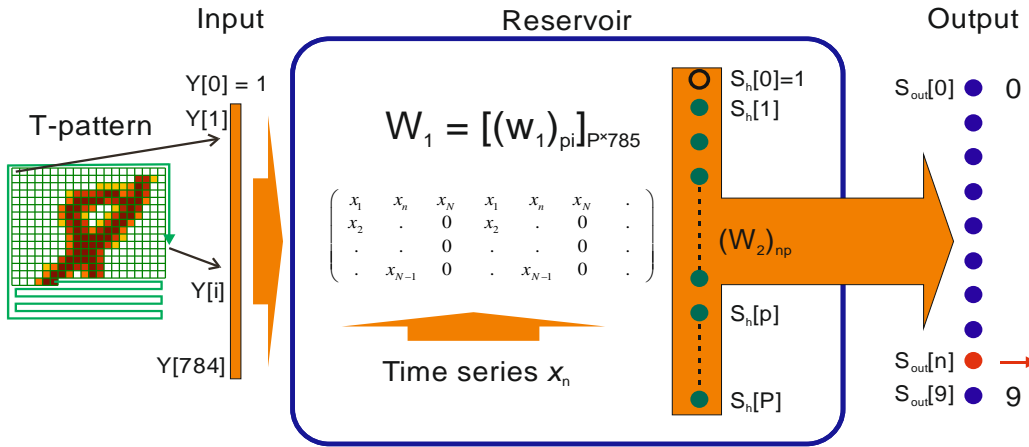


**Figure 1.** The LogNNet model structure for NNetEn calculation (copied from [21]).

The number of epochs  $Ep$  is the only control parameter of the algorithm. The classification accuracy of LogNNet shows the degree of chaos in the reservoir matrix and is defined as the NNetEn entropy measure, i.e.

$$\text{NNetEn}(Ep) = \frac{\text{Classification accuracy}}{100\%}. \quad (1)$$

The flowchart of NNetEn algorithm is shown in Table 1.

Table 1. NNetEn algorithm [21].

- 
1. Loading time series  $x_n$ .
  2. Loading the MNIST-10 database and the T-pattern-3 pattern [28] to convert input images into the vectors array  $Y$ .
  3. Initializing the initial values of weights and neurons.
  4. Constructing the reservoir matrix  $W_1$  using the given time series (Section 2.3.).
  5. Calculating the coefficients for normalization.
  6. Determining the number of training epochs  $Ep$ .
  7. Performing the training process of the LogNNet 784:25:10 network using a training set.
  8. Performing the testing process of the LogNNet 784:25:10 network with a test set and calculating the classification accuracy (1).
- 

In this article, we consider  $Ep = 100$  and  $\text{NNetEn} = \text{NNetEn}(100)$ .

## 2.2. Learning inertia calculation method

The concept of learning inertia (LI) is introduced in [21] for investigating the effect of  $Ep$  on the NNetEn value. For a given time series, the learning inertia with respect to epochs numbers  $Ep1$  and  $Ep2$  is defined as follows

$$LI(Ep1 / Ep2) = \frac{NNetEn(Ep2 \text{ epoch}) - NNetEn(Ep1 \text{ epoch})}{NNetEn(Ep2 \text{ epoch})}. \quad (2)$$

An analysis of the behavior of LI provides valuable information about the convergence of the learning process in neural networks models, which helps the researchers to discover additional features of chaotic signals. For example in [29] LI used for filtering the NNetEn signal ( $Ep1 = 20, Ep2 = 1$ ), and in [21] LI was the feature of the occurrence of weak chaos in the periodic component ( $Ep1 = 100, Ep2 = 400$ ).

In this article, we used  $Ep1 = 100$  and  $Ep2 = 400$ .

## 2.3. Techniques for filling reservoirs

In practice, it is difficult to obtain time series with element number  $N = 19625$ . Suppose we have a time series with  $N$  elements. If  $N > 19625$ , we must ignore  $N-19625$  elements of the time series and fill the matrix with the remaining elements. This case rarely occurs in real-world applications. When  $N < 19625$ , we provide six different filling methods based on row-wise and column-wise filling of the matrix. For example, we show a reduced matrix  $W_1$  filled with series  $x_n = n$ , where  $n$  varies from 1 to 9.

Method 1: Row-wise filling with duplication

In this method, the matrix  $W_1$  is filled row by row, doubling the row for subsequent elements, as described in Figure 2.

Method 2: Row-wise filling with an additional zero element

This method is similar to filling the matrix row by row. We consider the zero values for the remaining elements in the matrix row if the row cannot be filled with all the given time series elements. A schematic description and an example of this method can be found in Figure 3.

$$\left( \begin{array}{ccccccccc} x_1 & x_2 & \cdot & \cdot & x_n & \cdot & \cdot \\ x_{N-1} & x_N & x_1 & x_2 & \cdot & \cdot & x_n \\ \cdot & \cdot & x_{N-1} & x_N & x_1 & x_2 & \cdot \\ \cdot & \cdot & x_n & \cdot & \cdot & x_{N-1} & x_N \end{array} \right) \quad \begin{array}{c} 1 \rightarrow 2 \rightarrow 3 \rightarrow 4 \rightarrow 5 \rightarrow 6 \rightarrow 7 \\ \hline 8 \leftarrow 9 \quad 1 \quad 2 \quad 3 \quad 4 \quad 5 \\ 6 \quad 7 \quad 8 \quad 9 \quad 1 \quad 2 \quad 3 \\ 4 \quad 5 \quad 6 \quad 7 \quad 8 \quad 9 \quad 1 \end{array}$$

(a) (b)

**Figure 2.** (a) The structure of matrix filling method 1; (b) An example of a time series with 9 elements.

$$\left( \begin{array}{ccccccccc} x_1 & x_2 & \cdot & \cdot & x_n & \cdot & \cdot \\ x_{N-1} & x_N & 0 & 0 & 0 & 0 & 0 \\ x_1 & x_2 & \cdot & \cdot & x_n & \cdot & \cdot \\ x_{N-1} & x_N & 0 & 0 & 0 & 0 & 0 \end{array} \right) \quad \begin{array}{c} 1 \rightarrow 2 \rightarrow 3 \rightarrow 4 \rightarrow 5 \rightarrow 6 \rightarrow 7 \\ \hline 8 \leftarrow 9 \quad 0 \quad 0 \quad 0 \quad 0 \quad 0 \\ 1 \quad 2 \quad 3 \quad 4 \quad 5 \quad 6 \quad 7 \\ 8 \quad 9 \quad 0 \quad 0 \quad 0 \quad 0 \quad 0 \end{array}$$

(a) (b)

**Figure 3.** (a) The structure of matrix filling method 2; (b) An example of a time series with 9 elements.

### Method 3: Row-wise filling with time series stretching

This method fills the matrix row-wise and stretches the time series to  $N = 19625$ . The stretching method constructs a new time series  $\{z_n\}$  with  $N = 19625$  elements, whose elements are linear approximations between two adjacent points of the original time series  $\{x_n\}$ . Figure 4(a) shows a time series  $\{x_n\}$  with  $N = 100$  values. The stretched time series  $\{z_n\}$  is not unique. It gives almost the same results if we consider the time series as a record of a dynamic process (see Figure 4(b)). The detailed arrangement of the elements  $\{z_n\}$  near  $x_{28}$  is shown in Figure 4(c).

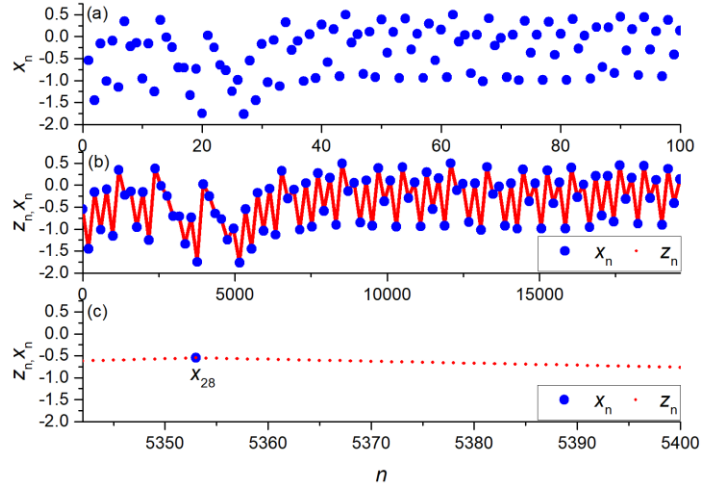


**Figure 4.** (a) The time series  $\{x_n\}$  with  $N = 100$  elements; (b) Stretching  $\{x_n\}$  into the time series  $\{z_n\}$  with  $N = 19625$  elements; (c) The detailed arrangement of elements  $\{z_n\}$  near  $x_{28}$ .

### Method 4: Column-wise filling with duplication

In this method, the matrix  $W_1$  is filled column by column, duplicating the columns for the subsequent elements, as shown in as shown in Figure 5.

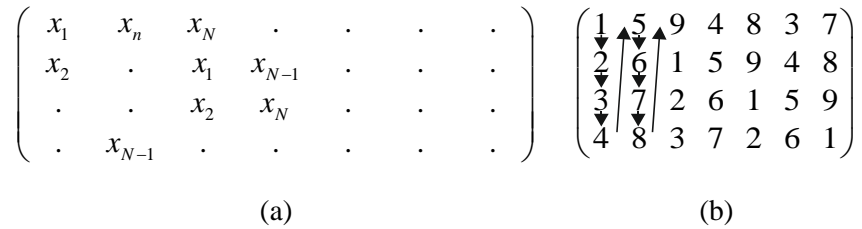


**Figure 5.** (a) The structure of matrix filling method 4; (b) An example of a time series with 9 elements.

### Method 5: Column-wise filling with an additional zero element

This method is similar to Method 2 where the column is considered instead of rows (see Figure 6).

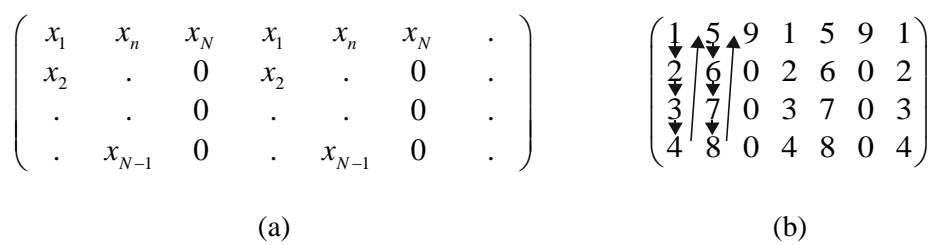


Figure 6. (a) The structure of matrix filling method 5; (b) An example of a time series with 9 elements.

## Method 6: Column-wise filling with time series stretching

In this method, the matrix is filled column by column, stretching the time series to  $N = 19625$ , as described in method 3.

## 3. Results

### 3.1. The effect of the length of the time series on the value of NNetEn

In order to investigate the efficiency and stability of the six matrix filling methods, these methods are applied to different types of time series, taking into account the variation of the number of elements  $N$ . The following time series are used to compare the different matrix filling methods.

Periodic discrete map:

$$x_n = A \cdot \sin\left(\frac{n \cdot 20\pi}{19625}\right). \quad (3)$$

Binary discrete map:

$$\begin{aligned} x_n &= n \bmod 2, \\ x_n &= (1, 0, 1, 0, 1, 0, 1, 0, 1, \dots). \end{aligned} \quad (4)$$

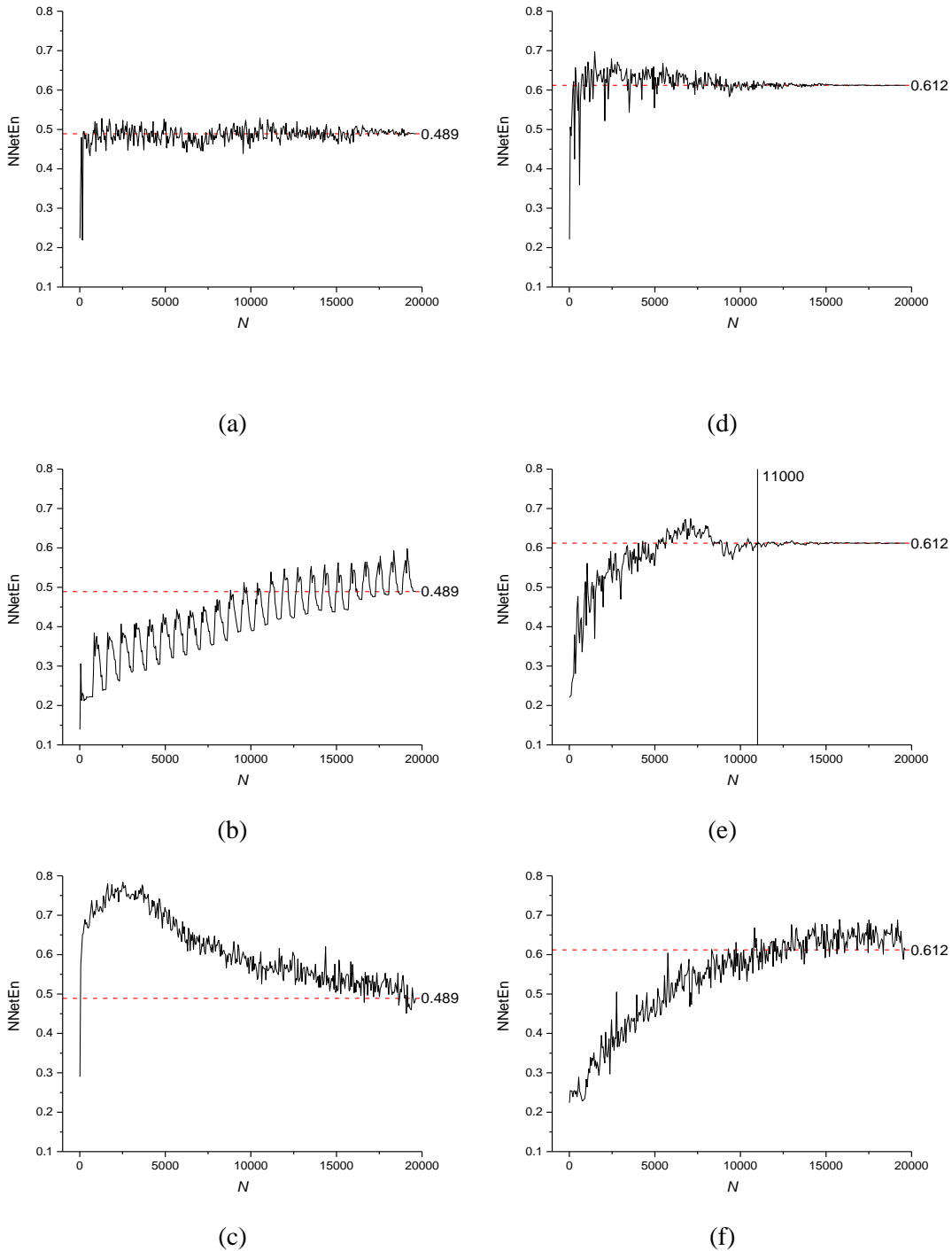
Logistic map:

$$x_{n+1} = r \cdot x_n \cdot (1 - x_n) \quad (5)$$

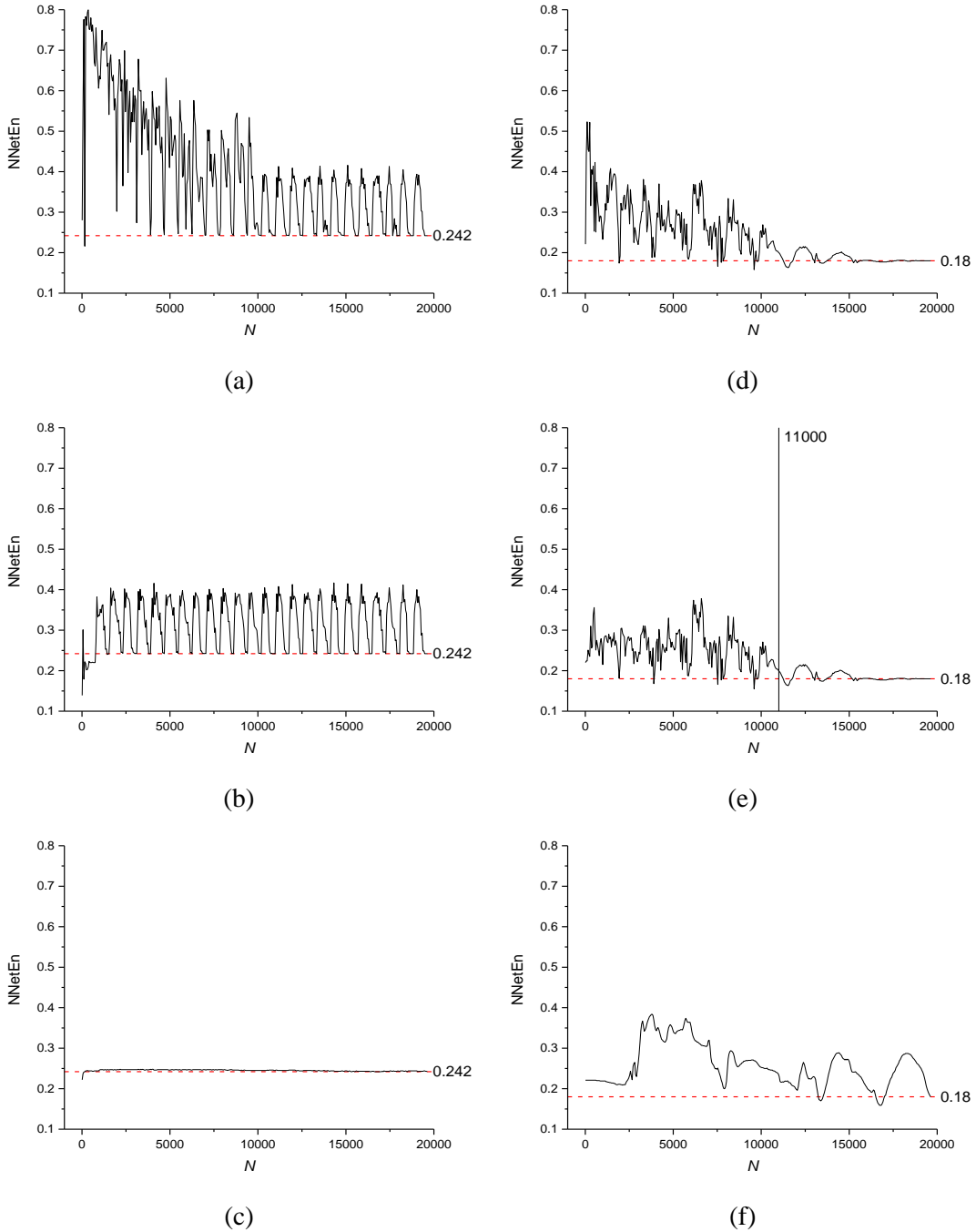
The epochs number is set to 100 in this subsection.

Figure 7 shows different matrix filling methods applied to NNetEn measures for a chaotic logistic map with  $r = 3.8$  and a varying number of elements  $N$ . The dashed red line shows the reference level corresponding to NNetEn at  $N = 19625$ . Reducing  $N$  below 19625 should not result in a significant change in entropy compared to the reference level. Method 5 is most stable for  $N \geq 11000$ , as the NNetEn values are virtually the same as the reference level. Method 1 is suitable for  $N < 11000$  because it has less variation and deviation from the reference level.

The NNetEn measures for sine periodic map (3) and a binary map (4) with a varying number of elements in the range  $N = 10, \dots, 19625$  are shown in Figure 8 and Figure 9 respectively.



**Figure 7.** The effect of time series length on NNetEn values for the logistic map (5) using different matrix filling methods: (a) Method 1; (b) Method 2; (c) Method 3; (d) Method 4; (e) Method 5; (f) Method 6.



**Figure 8.** The effect of time series length on NNetEn values for periodic time series (3) using different matrix filling methods: (a) Method 1; (b) Method 2; (c) Method 3; (d) Method 4; (e) Method 5; (f) Method 6.

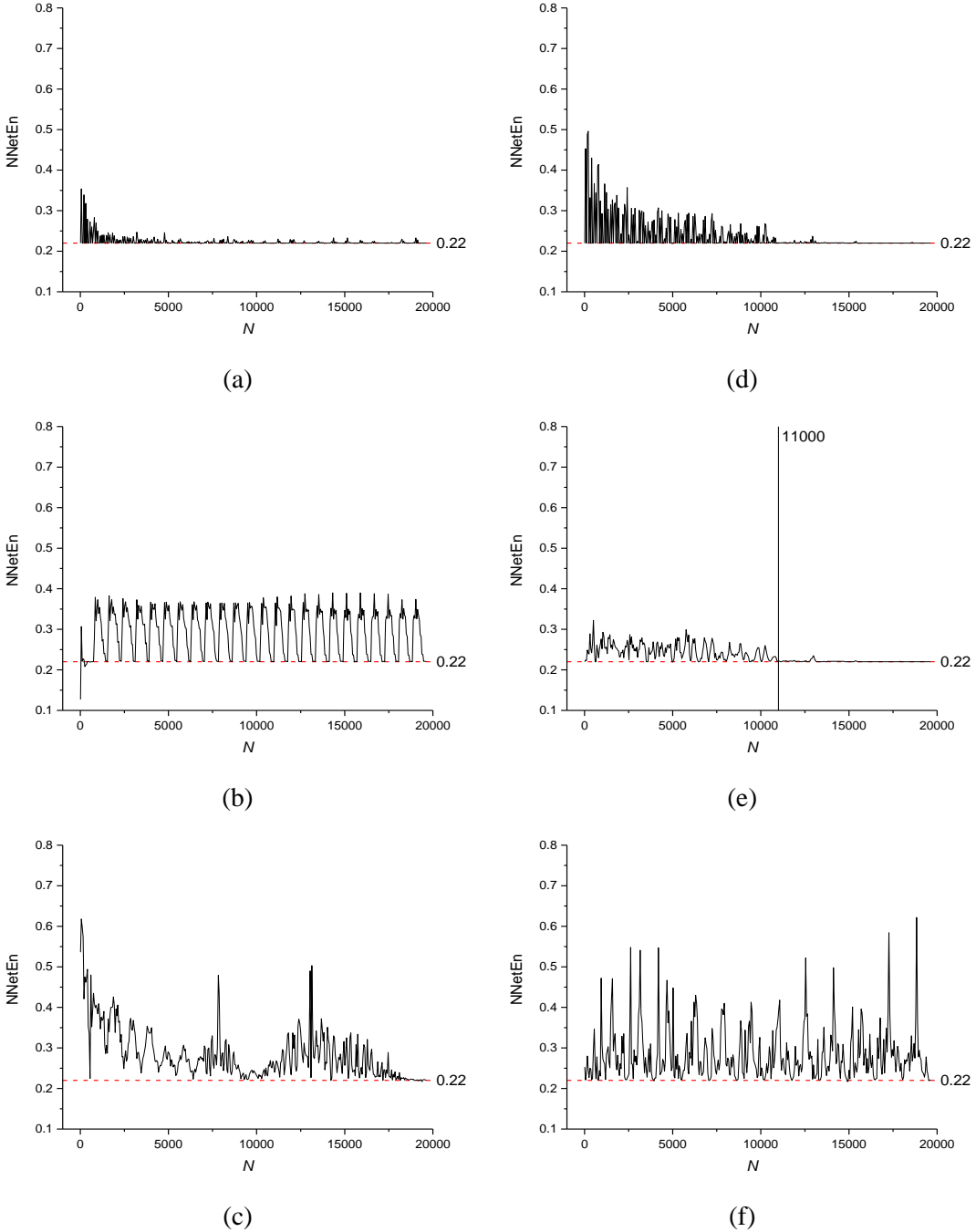


**Figure 9.** The effect of time series length on NNetEn values for binary time series (4) using different matrix filling methods: (a) Method 1; (b) Method 2; (c) Method 3; (d) Method 4; (e) Method 5; (f) Method 6.

Figure 8 shows that method 3 is the most suitable method for the periodic time series with  $N > 50$  because it has no fluctuations. Figure 9 shows that method 5 gives the most stable results for binary time series when  $N > 11000$ , and method 1 is suitable when the time series length is  $N > 50$ .

### 3.2. The effects of noise on the NNetEn measure

We consider the noisy signal in the form

$$y_n = x_n + z_n, \quad (6)$$

where  $x_n$  is the main signal given by Eqs. (3)- (5) and  $z_n$  is the noise. The random noise signal is formulated as

$$z_n = A \cdot (\text{random} - 0.5) + B, \quad (7)$$

where random is a random number between 0 and 1,  $A$  is amplitude of noise and  $B$  is the bias of noise signal. To investigate the effect of noise on NNetEn measure, we consider the following signal-to-noise ratio

$$SNR = 20 \cdot \log_{10} \left( \frac{A_{\text{signal}}}{A_{\text{noise}}} \right), \quad (8)$$

where  $A_{\text{signal}}$  and  $A_{\text{noise}}$  denote the amplitude of the main signal and the amplitude of noise respectively.

The matrix filling method 5 is considered as the main reservoir filling technique in NNetEn.

The NNetEn and learning inertia values for the main signals without noise and with different offset  $B$  can be found in Figure 10. In general, the dependencies have a bell-shaped form with a maximum of entropy at a certain bias value, and a minimum of LI corresponds to the maximum of NNetEn. For a binary signal, the entropy practically does not change. With an increase in the modulus of constant bias, a decrease in entropy is observed for a sinusoidal and logistic signal.

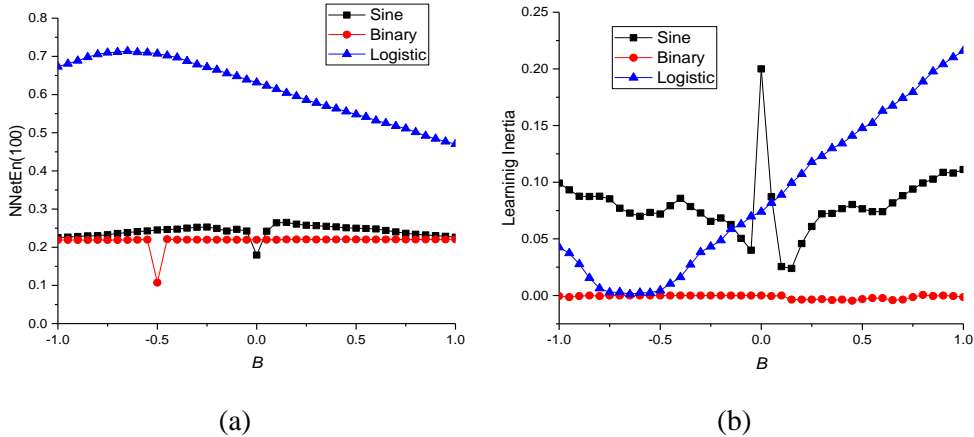


**Figure 10.** The NNetEn (a) and learning inertia (b) values for the main signals ( $A = 0$ ).

Different random signals are needed to detect the effects of noise on NNetEn. We use three different random signals in the form (7), whose first 100 elements are shown in Figure 11.

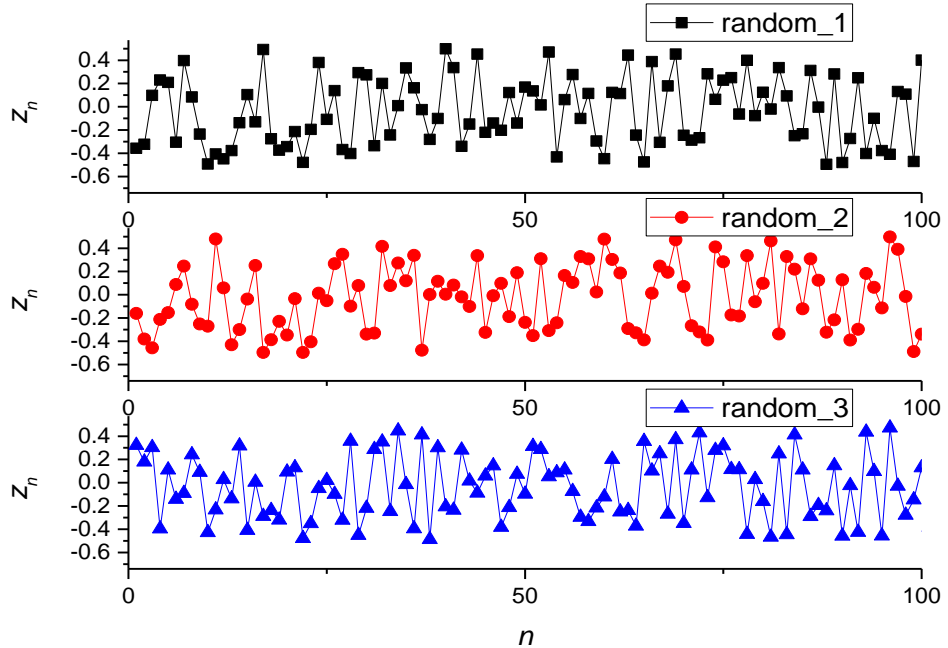


**Figure 11.** The first 100 elements of the random signals of the form (7) with  $A = 1$  and  $B = 0$ .

The properties of the random signals are listed in Table 2.

Table 2. The statistical properties of random signals.

Type of signal	$N$	Mean	Standard deviation	Sum	Minimum	Median	Maximum
random_1	19625	0.0015	0.28809	29.39545	-0.49999	0.00631	0.49999
random_2	19625	0.00242	0.28771	47.46514	-0.49999	0.00347	0.50000
random_3	19625	-0.00265	0.28832	-52.07462	-0.49993	-0.00575	0.50000

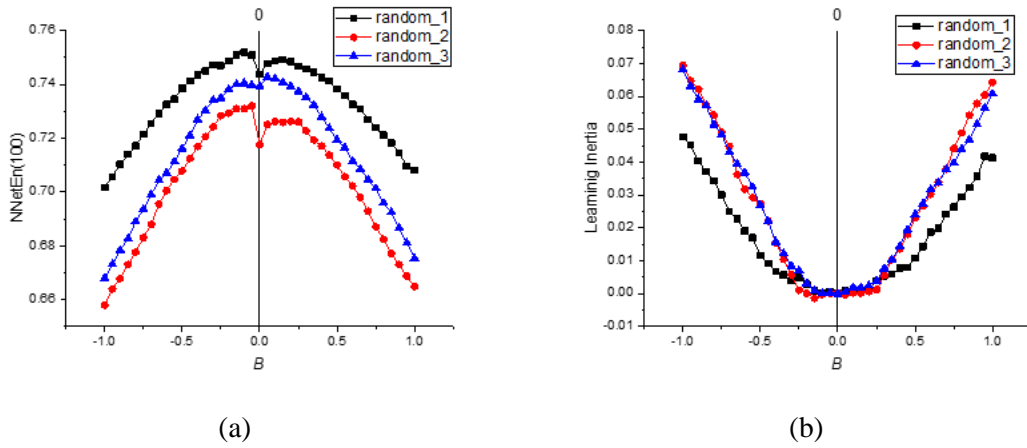


**Figure 12.** The NNetEn (a) and learning inertia (b) of random signals.

The NNetEn and learning inertia values for the random signals are shown in Figure 12. For all random signals, we find that the NNetEn value depends on parameter  $B$ , in the form of an inverted parabola (bell shape) with a maximum at  $B = 0$ , while the value of inertia has a minimum value at this point. It is clear that the mean value (Table 2) does not play a significant role since it has a small value for all three random signals. Their complexity determines the entropy of the signals at  $B = 0$ . Signal random\_1 has the highest entropy and the highest

complexity. The learning inertia is close to zero for all three signals and increases as  $|B|$  increases. The presence of a bell-shaped dependence of NNetEn on  $B$  is a universal phenomenon. This is because with an increase in the bias component  $B$ , the role of the chaotic components is weakened, and entropy decreases. At the same time, with a decrease in the role of the chaotic components, the value of LI increases. LI can be used as an indicator of the degree of chaos in terms of regularity in the system. This explains the increase of LI in the transition region mentioned in our previous work [21].

### 3.3. Influence of noise amplitude $A$ on the main signal

In this subsection, we consider the effects of noise scale  $A$  in NNetEn with  $B = 0$  in Eq. (7). Figure 13 shows how the shape of a sinusoidal signal changes as the noise amplitude increases from  $A = 0$  to  $A = 1$ . The SNR for  $A = 0.05, 0.1$ , and  $1$  is  $26.02$  dB,  $20$  dB, and  $0$  dB, respectively. The figure shows that an increase in the SNR leads to the loss of the periodic behavior of the signal. The effects of the amplitude noise on NNetEn for the periodic, binary, and chaotic time series are shown in Figure 14 through Figure 16. These figures show that the value of NNetEn is gradually increased by increasing the amount of noise while the learning inertia decreases. There is an upper bound for the SNR for each time series, so the NNetEn measure and LI remain unchanged for the smaller noise (higher SNR).

LI decreases with increasing noise because the chaotic property of the signal is directly related to the amount of noise. Training intensity increases as the chaotic behavior of the signal increases and, therefore, LI decreases. The value of LI reaches a pronounced maximum in areas of low noise. Also, LI experiences a marked decrease when noise amplitude  $A$  increases, especially at low values of  $A$ , where the signal is approximately periodic.

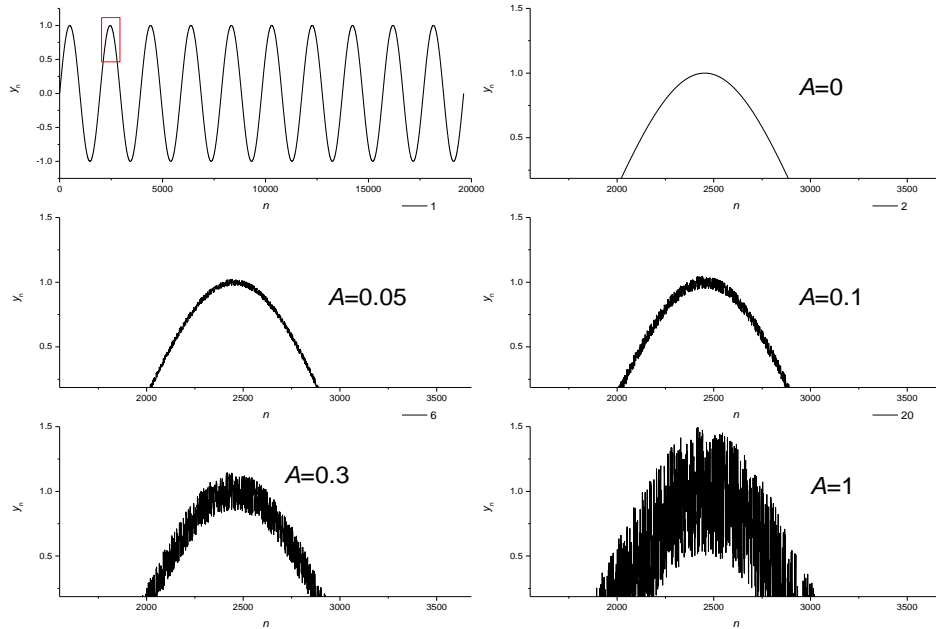


**Figure 13.** The effect of amplitude noise on sine periodic signal.

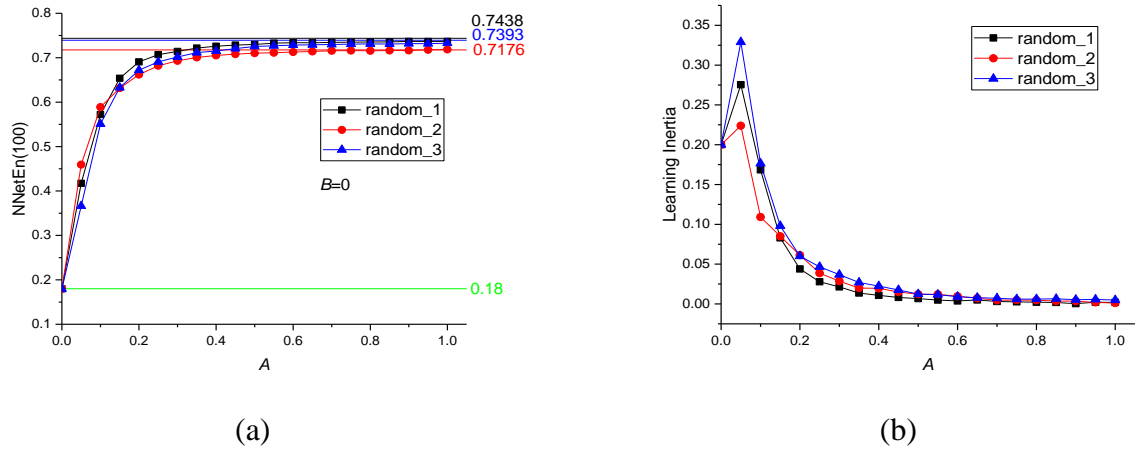


**Figure 14.** The NNetEn (a) and learning inertia (b) values of noisy sine periodic map where the offset is neglected.

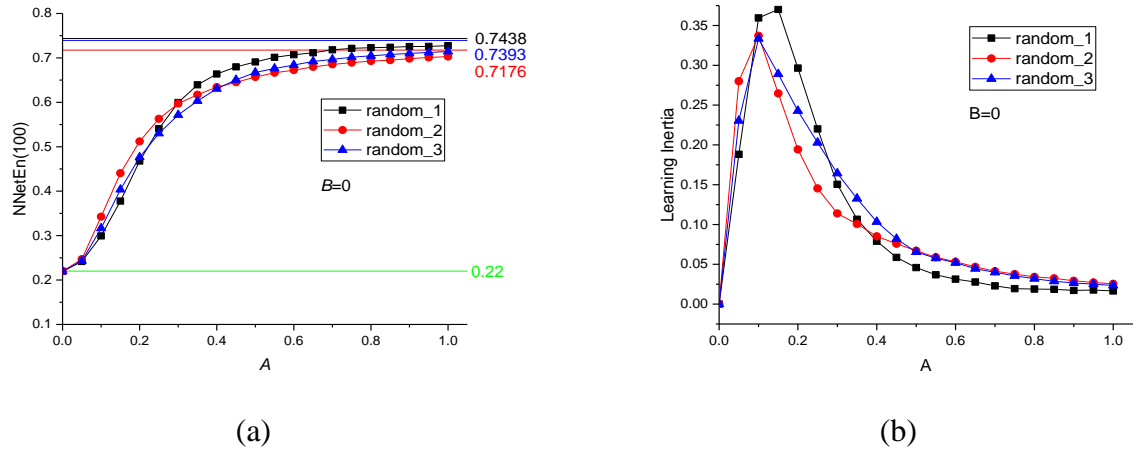


**Figure 15.** The NNetEn (a) and learning inertia (b) values of noisy binary map where the offset is neglected.

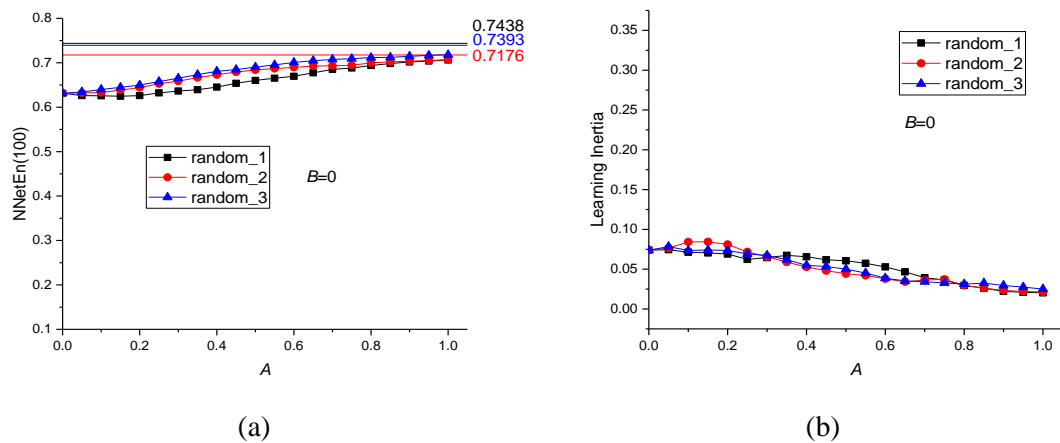


**Figure 16.** The NNetEn (a) and learning inertia (b) values of noisy logistic map where the offset is neglected.

The strongest change in NNetEn with increasing  $A$  is observed for the sine periodic map. When we increase  $A$  to 0.05, we have a  $\sim 100\%$  increase in NNetEn for sine,  $\sim 20\%$  for the binary map, and  $\sim 5\%$  for the logistic chaotic map. For the logistic chaotic map (Figure 16), NNetEn has a small variation because the signal is initially chaotic, and the addition of random noise slightly increases the irregularity. Therefore, the error in calculating NNetEn entropy does not exceed 10% for all types of signals when the SNR  $> 30$  dB. This opens up the possibility of measuring NNetEn of experimental signals with the presence of noise of various nature, white noise or 1/f noise, without the need for noise filtering.

### 3.4 The effect of offset $B$

In this subsection, we consider noise in the form of Eq. (7), where parameter  $A$  is fixed, and parameter  $B$  varies from 0 to 1 in 0.05 increments. To analyze the effects of offset  $B$ , the values of  $A$  are considered to be 0.05 and 0.3. The results are shown in Figures 17-19. NNetEn decreases in all figures. So, the stochastic property of the noisy signal decreases as offset  $B$  increases.

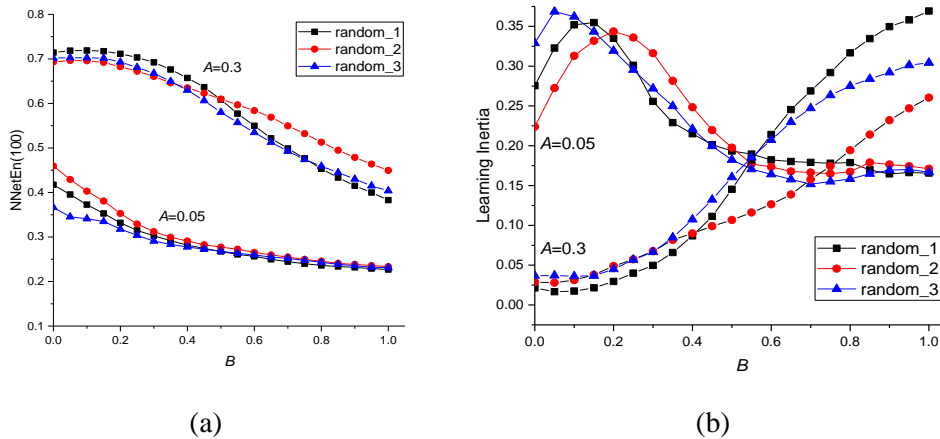


**Figure 17.** The NNetEn (a) and learning inertia (b) values of noisy sine periodic map for amplitude noise  $A = 0.05$  and 0.3 and different values of offset  $B$ .

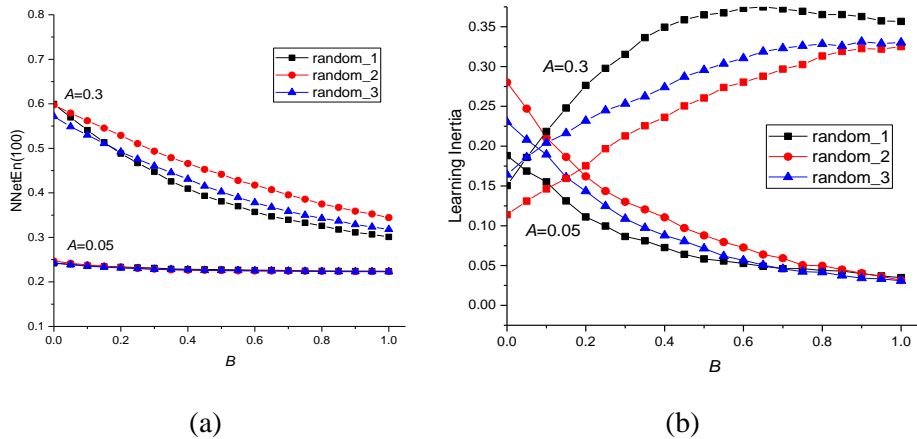


**Figure 18.** The NNetEn (a) and learning inertia (b) values of noisy binary map for amplitude noise  $A = 0.05$  and 0.3 and different values of offset  $B$ .

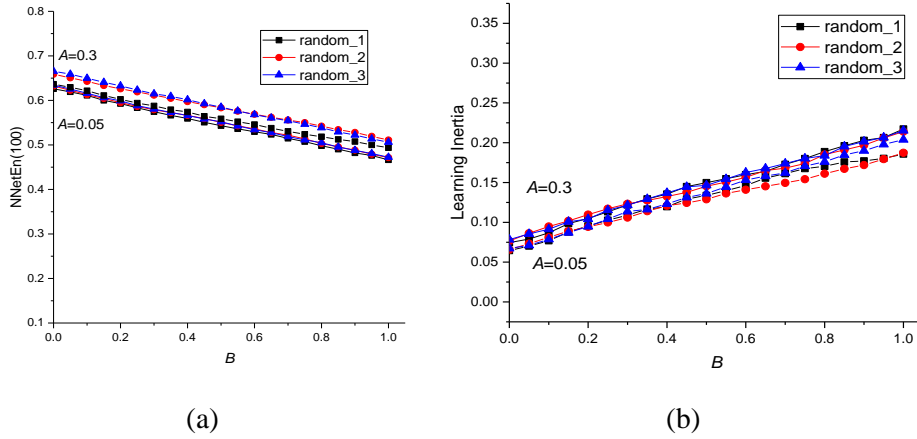


**Figure 19.** The NNetEn (a) and learning inertia (b) values of noisy logistic map for amplitude noise  $A = 0.05$  and  $0.3$  and different values of offset  $B$ .

Dependencies LI on  $B$  have more complex behavior than NNetEn. For a sinusoidal signal, we have maxima and minima, and for a logistic chaotic map, an increase in  $B$  leads to an increase in LI. An increase in  $B$  by 5% leads to a change in NNetEn of the order of 10%, so the value of  $B$  affects NNetEn less than  $A$ .

The relation between LI and  $B$  values is more complex than the relationship between NNetEn and  $B$ . For a sinusoidal signal, there are maxima and minima, and for a logistic chaotic map, an increase of  $B$  leads to an increase of LI. A 5% increase in  $B$  results in a change in NNetEn of the order of 10%, so the value of  $B$  affects NNetEn less than  $A$  does.

#### 4. Discussion and conclusion

Entropy is a fundamental concept of information technology. Entropy measures are widely used in time series analysis. Conventional entropy measures such as Shannon entropy, approximate entropy, and multiscale entropy have drawbacks. For example, approximate entropy depends on two parameters, which reduces its efficiency, Shannon entropy, and multiscale entropy are sensitive to the length of the time series. Recently, the NNetEn entropy measure is introduced to overcome these difficulties. The NNetEn algorithm contains a reservoir matrix with  $N = 19625$  elements, which the given time series should fill. Many practical time series have less than 19625 elements. This paper proposes six matrix filling methods to construct the reservoir matrix when the time series has less than 19625 elements. To compare the efficiency of the different matrix filling methods, the methods are applied to chaotic, periodic and binary time series with the number of elements in the range  $N = 10, \dots, 19625$ . The results show that method 1 is suitable for chaotic series with arbitrary length and binary time series with short length  $N \geq 50$ ; method 3 is the most suitable method for the periodic time series with short length  $N \geq 50$ . Method 5 gives the most stable results for time series with a length of more than 11000. Thus, to calculate entropy, need to specify the number of training epochs  $Ep$  and the most suitable method to calculate it.

The effects of noise on NNetEn for chaotic, periodic and binary time series are investigated. The results show that the error in NNetEn entropy calculation does not exceed 10% when the SNR exceeds 30 dB. This opens the possibility to measure the NNetEn of experimental signals in the presence of noise of different types, white noise or 1/f noise, without the need for noise filtering.

## References

- [1] J. Li, P. Shang, X. Zhang, Financial time series analysis based on fractional and multiscale permutation entropy, *Commun. Nonlinear Sci. Numer. Simul.* 78 (2019) 104880. <https://doi.org/10.1016/j.cnsns.2019.104880>.
- [2] A.S. Minhas, P.K. Kankar, N. Kumar, S. Singh, Bearing fault detection and recognition methodology based on weighted multiscale entropy approach, *Mech. Syst. Signal Process.* 147 (2021) 107073. <https://doi.org/10.1016/j.ymssp.2020.107073>.
- [3] Y.T. Ai, J.Y. Guan, C.W. Fei, J. Tian, F.L. Zhang, Fusion information entropy method of rolling bearing fault diagnosis based on n-dimensional characteristic parameter distance, *Mech. Syst. Signal Process.* 88 (2017) 123–136. <https://doi.org/10.1016/j.ymssp.2016.11.019>.
- [4] J.S. Ra, T. Li, L. Yan, Improving Epileptic Seizure Prediction, *Sensors* (Switzerland) 21 (2021) 7972.
- [5] R. Zavala-yoe, R.A. Ramirez-mendoza, L.M. Cordero, Entropy measures to study and model long term simultaneous evolution of children in Doose and Lennox – Gastaut syndromes, 15 (2016) 205–221. <https://doi.org/10.1142/S0219635216500138>.
- [6] F. Benedetto, L. Mastroeni, P. Vellucci, Modeling the flow of information between financial time-series by an entropy-based approach, *Ann. Oper. Res.* 299 (2021) 1235–1252. <https://doi.org/10.1007/s10479-019-03319-7>.
- [7] F. Nie, P. Zhang, J. Li, D. Ding, A novel generalized entropy and its application in image thresholding, *Signal Processing* 134 (2017) 23–34. <https://doi.org/10.1016/j.sigpro.2016.11.004>.
- [8] I. Aaron Oludehinwa, O. Isaac Olusola, O. Segun Bolaji, O. Olayinka Odeyemi, A. Ndzi Njah, Magnetospheric chaos and dynamical complexity response during storm time disturbance, *Nonlinear Process. Geophys.* 28 (2021) 257–270. <https://doi.org/10.5194/NPG-28-257-2021>.
- [9] M. Zanin, F. Olivares, series, *Commun. Phys.* (2021). <https://doi.org/10.1038/s42005-021-00696-z>.
- [10] A. Delgado-Bonal, A. Marshak, Approximate entropy and sample entropy: A comprehensive tutorial, *Entropy* 21 (2019) 541. <https://doi.org/10.3390/e21060541>.
- [11] Z. Chen, Y. Li, H. Liang, J. Yu, Improved Permutation Entropy for Measuring Complexity of Time Series under Noisy Condition, 2019 (2019).
- [12] H.B. Xie, T. Guo, Fuzzy entropy spectrum analysis for biomedical signals de-noising, 2018 IEEE EMBS Int. Conf. Biomed. Heal. Informatics, BHI 2018. 2018–Janua (2018) 50–53. <https://doi.org/10.1109/BHI.2018.8333367>.
- [13] S. Chatterjee, S.C. Chapman, B.M. Lunt, M.R. Linford, Using cross-correlation with pattern recognition entropy to obtain reduced total ion current chromatograms from raw liquid chromatography-mass spectrometry data, *Bull. Chem. Soc. Jpn.* 91 (2018) 1775–1780. <https://doi.org/10.1246/BCSJ.20180230>.
- [14] S.D. Na, Q. Wei, K.W. Seong, J.H. Cho, M.N. Kim, Noise reduction algorithm with the soft thresholding based on the Shannon entropy and bone-conduction speech cross- correlation bands, *Technol. Heal. Care.* 26 (2018) 281–289. <https://doi.org/10.3233/THC-174615>.
- [15] Z. Wang, J. Wang, Z. Zhao, R. Wang, A novel method for multi-fault feature extraction of a gearbox under strong background noise, *Entropy* 20 (2018). <https://doi.org/10.3390/e20010010>.
- [16] M.U. Ahmed, D.P. Mandic, Multivariate Multiscale Entropy Analysis, 19 (2012) 91–94.
- [17] S. Simons, P. Espino, D. Abásolo, Fuzzy Entropy analysis of the electroencephalogram in patients with Alzheimer’s disease: Is the method superior to Sample Entropy?, *Entropy* 20 (2018) 1–13. <https://doi.org/10.3390/e20010021>.
- [18] H. Niu, J. Wang, Quantifying complexity of financial short-term time series by composite multiscale entropy measure, *Commun. Nonlinear Sci. Numer. Simul.* 22 (2015) 375–382. <https://doi.org/10.1016/j.cnsns.2014.08.038>.
- [19] S. Molavipour, H. Ghouchian, G. Bassi, M. Skoglund, Neural estimator of information for time-series data with dependency, *Entropy* 23 (2021) 1–28. <https://doi.org/10.3390/e23060641>.
- [20] S. De Wu, C.W. Wu, K.Y. Lee, S.G. Lin, Modified multiscale entropy for short-term time series analysis, *Phys. A Stat. Mech. Its Appl.* 392 (2013) 5865–5873. <https://doi.org/10.1016/j.physa.2013.07.075>.

- [21] A. Velichko, H. Heidari, A Method for Estimating the Entropy of Time Series Using Artificial Neural Networks, *Entropy*. 23 (2021). <https://doi.org/10.3390/e23111432>.
- [22] M.W.F. Id, B. Grimm, EntropyHub : An open-source toolkit for entropic time series analysis, (2021) 1–20. <https://doi.org/10.1371/journal.pone.0259448>.
- [23] X. Zhao, M. Ji, N. Zhang, P. Shang, Permutation transition entropy: Measuring the dynamical complexity of financial time series, *Chaos, Solitons and Fractals*. 139 (2020). <https://doi.org/10.1016/j.chaos.2020.109962>.
- [24] J. Keum, P. Coulibaly, Sensitivity of Entropy Method to Time Series Length in Hydrometric Network Design, *J. Hydrol. Eng.* 22 (2017) 4017009. [https://doi.org/10.1061/\(asce\)he.1943-5584.0001508](https://doi.org/10.1061/(asce)he.1943-5584.0001508).
- [25] G. Litak, R. Taccani, R. Radu, K. Urbanowicz, J.A. Hołyst, M. Wendeker, A. Giadrossi, Estimation of a noise level using coarse-grained entropy of experimental time series of internal pressure in a combustion engine, *Chaos, Solitons & Fractals*. 23 (2005) 1695–1701. <https://doi.org/10.1016/j.chaos.2004.06.057>.
- [26] J.S. Richman, J.R. Moorman, Physiological time-series analysis using approximate entropy and sample entropy maturity in premature infants Physiological time-series analysis using approximate entropy and sample entropy, *Am. J. Physiol. Hear. Circ. Physiol.* 278 (2000) H2039–H2049.
- [27] Y.H. Pan, Y.H. Wang, S.F. Liang, K.T. Lee, Fast computation of sample entropy and approximate entropy in biomedicine, *Comput. Methods Programs Biomed.* 104 (2011) 382–396. <https://doi.org/10.1016/j.cmpb.2010.12.003>.
- [28] A. Velichko, Neural Network for Low-Memory IoT Devices and MNIST Image Recognition Using Kernels Based on Logistic Map, *Electronics*. 9 (2020) 1432. <https://doi.org/10.3390/electronics9091432>.
- [29] I.A. Oludehinwa, A. Velichko, B.O. Ogunsua, O.I. Olusola, O.O. Odeyemi, A.N. Njah, O.T. Ologun, Dynamical complexity response in Traveling Ionospheric Disturbances across Eastern Africa sector during geomagnetic storms using Neural Network Entropy., *Earth Sp. Sci. Open Arch.* (2022) 46. <https://doi.org/10.1002/essoar.10510393.1>.